The Holocene 16,5 (2006) pp. 675–684

Holocene environmental change inferred from a high-resolution pollen record, Lake Zhuyeze, arid China

Fa-Hu Chen,[1,2*] Bo Cheng,[1] Yan Zhao,[1] Yan Zhu[1†] and David B. Madsen[3]

([1]CAEP, Key Laboratory of Western China's Environmental System (Ministry of Education), Lanzhou University, Lanzhou 730000, China; [2]Key Laboratory of Desert and Desertification, CAREERI, Chinese Academy of Science, Lanzhou 730000, China; [3]Texas Archeological Research Laboratory, University of Texas, Austin TX 78712, US)

Received 9 May 2005; revised manuscript accepted 21 November 2005

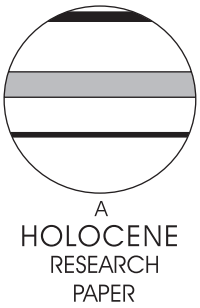

Abstract: A high-resolution pollen record, *c.* 50 yr/sample, from terminal lake sediments in the Shiyang River drainage basin on the present margin of the summer monsoon was used to reconstruct vegetation and climate history during the Holocene. Forest trees from mountainous areas of the drainage, including *Sabina*, *Picea* and *Pinus*, dominated pollen assemblages in the early Holocene (11.6–7.1 cal. ka). In the mid-Holocene (7.1–3.8 cal. ka) desert and steppe shrubs and herbs around the lake, including *Nitraria*, Poaceae, Compositae and *Artemisia*, were dominant. The late Holocene (3.8–0 cal. ka) was again dominated by alternation of *Pinus–Sabina* tree pollen and desert-steppe pollen. The early Holocene forest expansion in the mountains and subsequent increase in the river transport of tree pollen corresponds with maximum precipitation during the East Asian summer monsoon maximum. The timing of these changes in our record from arid China is different from that of East China, where the Holocene monsoon maximum appeared in the middle Holocene. This difference indicates that the extent and development of summer monsoon circulation in the Holocene was complex. Changes in the pollen record appear to show pervasive and persistent centennial- to millennial-scale oscillations throughout both wet and dry periods of the Holocene. Our results imply the continental interior was sensitive to changing moisture conditions and responsive to Holocene climatic events.

Key words: Arid inland China, pollen assemblages, Holocene monsoon maximum, arid events, millennial and centennial climate variations.

Introduction

Some previous studies have suggested that climate was stable during the Holocene (Jouzel *et al.*, 1987; Dansgaard *et al.*, 1993; Von Grafenstein *et al.*, 1999), while other research indicates it was unstable, with periodic fluctuations (O'Brien *et al.*, 1995) and with rapid changes (Stager and Mayewski, 1997; Bond *et al.*, 1997). These rapid centennial- to millennial-scale changes have been recorded in high-latitude regions of the Northern Hemisphere in sediments from the North Atlantic (Bianchi and McCave, 1999) and from North American lakes (Campbell *et al.*, 1998), and may also exist in most parts of the world (Mayewski *et al.*, 2004). However, these records of Holocene climatic instability are not numerous and are especially lacking for the arid regions of the Eurasian continent.

The prevalent opinion about Holocene climate change in China is that the Holocene Optimum, defined by warm temperatures and abundant precipitation, occurred in the mid-Holocene (Shi *et al.*, 1994). However, some studies have discovered that the Holocene Optimum was asynchronous (Wu *et al.*, 1994; An *et al.*, 2000; He *et al.*, 2004) and occurred during the early Holocene in areas of arid and semi-arid western China influenced by the summer monsoon (Wang *et al.*, 1998; Yang, 2000; Liu *et al.*, 2002; Madsen *et al.*, 2003). Some dry events have been found during the mid-Holocene (Li *et al.*, 2000; Chen, F.H., *et al.*, 2003) along the present summer monsoon margin, despite evidence for increased precipitation during the mid-Holocene in the south part of

*Author for correspondence (e-mail: fhchen@lzu.edu.cn)
†Deceased.

10.1191/0959683606hl951rp

the western Chinese Loess Plateau (An *et al.*, 2003). More work, therefore, is needed to assess the stability of Holocene climates and the timing of the Holocene Optimum in the summer monsoon margin area.

The Shiyang River drainage lies on the present margin of the East Asian summer monsoon and arid western China (Figure 1), an area where climate is strongly influenced both by the East Asian Monsoon and prevailing Westerlies. Ecosystems in the region are, thus, sensitive to climate change (Feng *et al.*, 2000). Pollen records from lakes in this region are correspondingly sensitive to monsoonal variations and have been the focus of a number of studies. Studies of pollen transportation to the terminal lakes along the drainage, together with vegetational reconstructions using pollen assemblages (Cheng, 2002; Zhu, 2002; Zhu *et al.*, 2002, 2003; Cheng *et al.*, 2004), have found that the pollen record in this drainage is indicative of climate change cycles at millennial scales during the early Holocene (Chen *et al.*, 2001; Zhu *et al.*, 2002). Holocene climatic variability was also found at an outcrop section along the Hongshui River (Zhang *et al.*, 2000; Ma *et al.*, 2004), a tributary in the Shiyang River drainage basin. However, this outcrop section can only reliably be used to reconstruct climatic history between 8 cal ka and 3 cal ka BP. In this study, we selected a continuous lake sediment section from the presently dry terminal lake (Lake Zhuyeze) of the Shiyang River drainage in arid western China to reconstruct the entire Holocene climate history using a high resolution (*c.* 50 yr/sample) pollen record.

Study region and site

The Shiyang River drainage, 300 km long with an area of 41 163 km^2, is located on the northern margin of the Tibetan Plateau. The river originates from the northern side of the Qilian Mountains, flows northward through fluvial/alluvial fan plain and Gobi, and forms Lake Zhuyeze in its lower reaches between the Tengger and Badain Jaran deserts, two of the major sand deserts in northwest China (Figure 1). During the late Pleistocene and early Holocene there was an extensive lake at the end of the drainage (Pachur *et al.*, 1995; Shi *et al.*, 2002), but by the 1950s, the palaeolake was completely dry as a result of human activity (Chen *et al.*, 1999). Annual precipitation in the drainage, of which about 80% falls from June to September, varies from less than 100 mm in the lowlands to over 500 mm in the mountains, with two-thirds of the river's runoff originating in the mountainous region. The average meltwater from glaciers and snow is a negligible 3.8% of the total river runoff in the Shiyang River drainage (Chen and Qu, 1992). The distribution of vegetation in the drainage is strongly related to elevation (Figure 1): Zone 1, a perennial snow and glacial zone (>4500 m); Zone 2, an alpine cushion-like vegetation zone (4500–3800 m); Zone 3, an alpine meadow zone (3800–3500 m); Zone 4, an alpine shrub zone (3500–3100 m); Zone 5, a *Picea* and *Sabina* forest zone (3100–2500 m); Zone 6, a mountainous grassland zone (2500–2350 m); and Zone 7, a desert grass (2350–2000 m) and a Gobi/sand desert (<2000 m) zone (Huang, 1997).

The section we studied, a 700-cm deep excavation at an elevation of 1320 m near Sanjiaocheng (SJC) at latitude 39°00′38″N, longitude 103°20′25″E, is located on the western part of the lake (Figure 1). Because of recent desertification, the present land surface is covered by eolian sand. Samples were taken every 2 cm at the section for analyses of various environmental proxies. The upper 232 samples were used for pollen analysis, with a time resolution of about 50 yr/sample. Twelve samples were taken for radiocarbon age estimates at lithological boundaries and from organic-rich layers. Eight of these samples date to the Holocene period (Figure 2).

Pollen analysis method

Standard techniques were employed for pollen extraction and analysis with some modifications (Li *et al.*, 1995). For silty clay, 60–80 g samples were taken for laboratory analysis, while for silt and sand, 100–120 g samples were taken. The procedure included sample washes in HCl and HF and filtering through 6 μm mesh. Two or three tablets of *Lycopodium* spores (about 12 524 spores/tablet) were added to each sample in order to

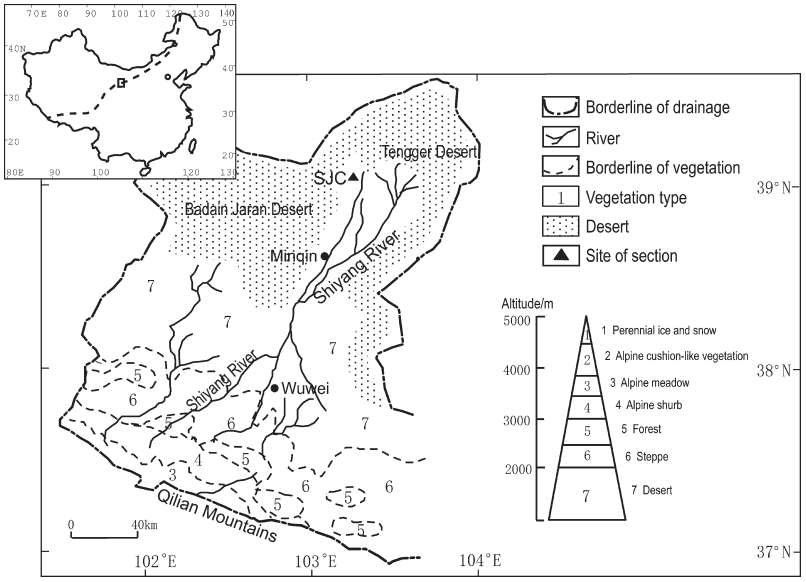

Figure 1 Map showing the geographical location of the study area (inset) and the northern limit of the Asian summer monsoon (dotted line; Gao *et al.*, 1962) in China and the SJC section in the Shiyang River drainage. The spatial distribution of vegetation types is marked by numbers 1–7, and the altitude distribution of vegetation types is shown in the inset triangle

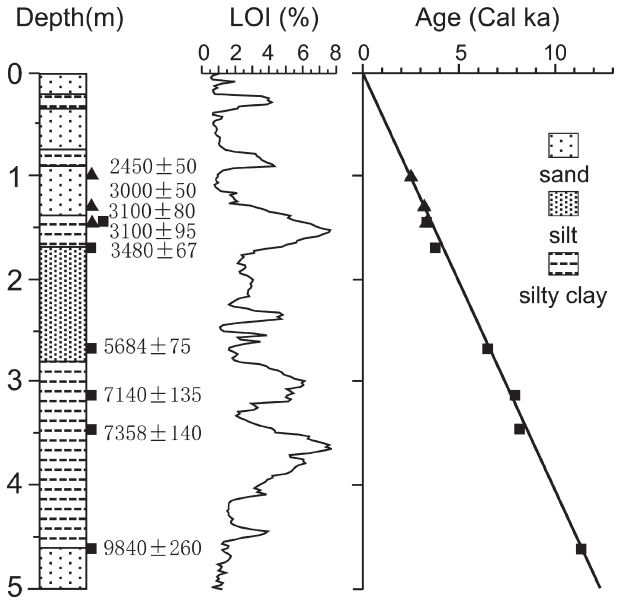

Figure 2 Stratigraphy and chronology of the SJC section. The carbon reservoir corrected radiocarbon dates are marked beside the lithological bar (solid squares, ^{14}C age for bulk organic matter; solid triangles, ^{14}C age for charcoal). The relationship of calibrated ages with depth is nearly linear during the Holocene. Loss-on-ignition (LOI) with depth (Chen *et al.*, 2001) is also shown

estimate the pollen concentration. Over 300 pollen grains and spores per sample were counted, except for very low concentration samples in the mid-section. For these, only about 150 pollen grains and spores of terrestrial vegetation were identified and counted.

Results

Lithology

The section is composed of continuous deposits consisting of silty clay, silt, and sand with 2–5 cm thick black layers with high organic matter content. Based on the lithological variations evident in the Loss-On-Ignition (LOI) curve (Figure 2; Chen *et al.*, 2001), the entire section can be divided from top to bottom as follows:

- 0–21 cm: reddish yellow sand containing gravel, lacustrine and fluvial deposits covered by aeolian sand at the surface.
- 21–168 cm: green-grey silt and silty clay of lacustrine sediment with two interbedded fine sand layers at 36–76 cm and 90–140 cm depths which have low LOI content (Figure 2).
- 168–280 cm: grey fine sand and silt layer with 3–5 cm thick dark clay silt layers.
- 280–460 cm: dark grey silt and silty clay of lacustrine deposition. The radiocarbon age at the lower limit of the unit is 9840±260 BP (LZU00-28), and marks the beginning of the Holocene at the section.
- 460–532 cm: light grey silt and fine sand.
- 532–600 cm: two silty clay layers interbedded with a layer of yellowish aeolian sand at 544–562 cm.
- 600–700 cm: yellowish aeolian sand with clear cross-stratified structure.

High measures of LOI, a proxy of organic carbon matter, and $CaCO_3$ generally coincide with fine grain-size layers such as clay or silty clay layers.

^{14}C dates and chronoloy

Radiocarbon dating was conducted by conventional ^{14}C method on five bulk organic matter samples at LZU radiocarbon laboratory of Lanzhou University, China, and by accelerator mass spectrometer (AMS) on picked charcoal samples at the Beta radiocarbon laboratory of the USA and the Gif radiocarbon laboratory of France. The radiocarbon ages measured in LZU are adjusted to use a 5568-yr half-life of radiocarbon. All ^{14}C ages were carbon-13 isotope adjusted. One sample at a depth of 1.3 m was dated using both bulk organic matter and charcoal. The radiocarbon age from charcoal material is about 3100 yr BP, while that from organic matter is about 3640 yr BP. We consider this age difference of about 540 years to be the carbon reservoir effect present in the lake because the charcoal radiocarbon age likely represents the true age of deposition. Therefore, we subtracted 540 years from all the measured radiocarbon dates from organic matter samples. The corrected radiocarbon dates, as marked in Figure 2, were then calibrated into calendar years following Stuiver and Reimer (1993). These calibrated ages have a nearly linear relationship with depth (Figure 2). A detailed age model is reported in Zhu (2002) and Chen *et al.* (2001). In this study, we focus only on the Holocene period at the section and adopt Zhu's age model to establish our Holocene age sequence. As a result, all ages in the following text are calendar years (BP) or thousand calendar years (ka).

Pollen diagram

Over 50 plant taxa were identified in the samples, but only the main taxa are shown in Figure 3. To show the local and regional vegetational variation more clearly, Figure 4 is a pollen diagram without pollen from montane vegetation and aquatic plants. Based on the relationship between pollen assemblages and the distribution of modern vegetation in the drainage (Zhu *et al.*, 2003; Cheng *et al.*, 2004), all pollen taxa can be divided into three broad ecological groups as shown on Figure 5. There are: (1) pollen taxa representing high-elevation vegetation, especially that from forest zones, include *Sabina*, *Picea*, *Pinus*, *Betula*, *Corylus*, *Ulmus*, *Quercus* and *Selaginella*; (2) regional vegetation taxa, derived from steppe vegetation common across the whole drainage basin, are represented by Rosaceae, Leguminosae, Rhamnaceae, Poaceae, Compositae, Chenopodiaceae, Cyperaceae, *Artemisia* and *Polygonum*; (3) pollen taxa from the lower reaches of the drainage, primarily xerophytes from the desert vegetation zones and marsh vegetation from the lake margin, include taxa such as *Nitraria*, *Calligonum*, *Ephedra*, *Zygoghyllaceae*, Plumbaginaceae, Elaeagnaceae and *Typha*.

The pollen assemblages of the SJC section can be divided into three zones.

Zone I: (460–282 cm; 11.6–7.1 ka)

Conifer taxa dominate the pollen assemblages, and *Sabina*, *Picea* and *Pinus* contribute 50–90% of the pollen sum (Figure 3). The peak values of *Sabina* and *Picea* alternate. In the high-elevation pollen group, broadleaf tree pollen has values of 1–11%, and the fern spores reach 4%. Shrub plant pollen and steppe taxa constitute 1–12% and 2–18%, respectively. *Nitraria* pollen is the primary local taxon, making up 0.2–9% of the total. *Typha* pollen is the main component of aquatic pollen, but with a low percentage value, lower than 1%. This zone is characterized by relatively high pollen concentrations, with a peak value of 2000–3000 grains/g and a mean value of 400–1500 grains/g. The concentration values are also highly variable. The percentages and concentration values of *Picea*

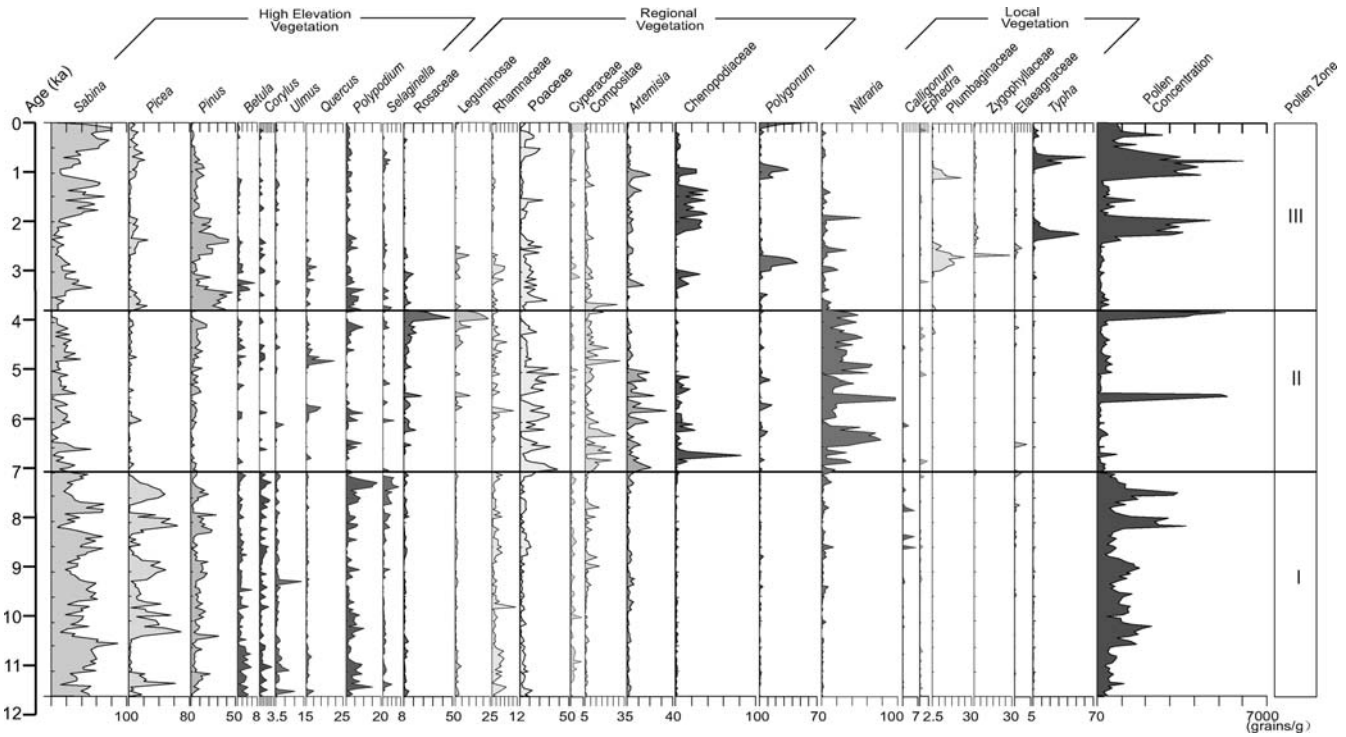

Figure 3 Pollen percentage diagram, pollen concentrations and pollen zones at the SJC section plotted with calibrated age

and *Pinus* pollen and fern spores change in concert, while the concentrations of *Sabina*, regional vegetation and xerophyte pollen taxa show either little change or even decrease despite an increase in their percentages (Figure 3).

Zone II: (282–152 cm; 7.1–3.8 ka)

This zone is characterized by high percentages of desert and steppe shrub and herb pollen (Figures 3–5). Regional vegetation and xerophyte pollen (Figure 4) are the main components, while conifer pollen is much lower than in Zone I (Figure 5). The percentages of regional pollen types are higher than in Zone I and Zone III. Shrub pollen has values up to 10%, but reaches 70% in some layers (such as the 224–218 cm layer, around 5.5 ka); Steppe taxa are consistently about 20% of the total pollen sum. *Nitraria* pollen increases markedly with the highest value reaching 90%. Aquatic pollen disappears almost completely (Figure 3). Pollen concentrations reach their lowest values in this section, except for very high values in two periods (Figures 3–5). These remarkably high pollen concentrations, with values reaching 5000 grains/g, are due to xerophyte pollen such as *Nitraria* (Figure 4).

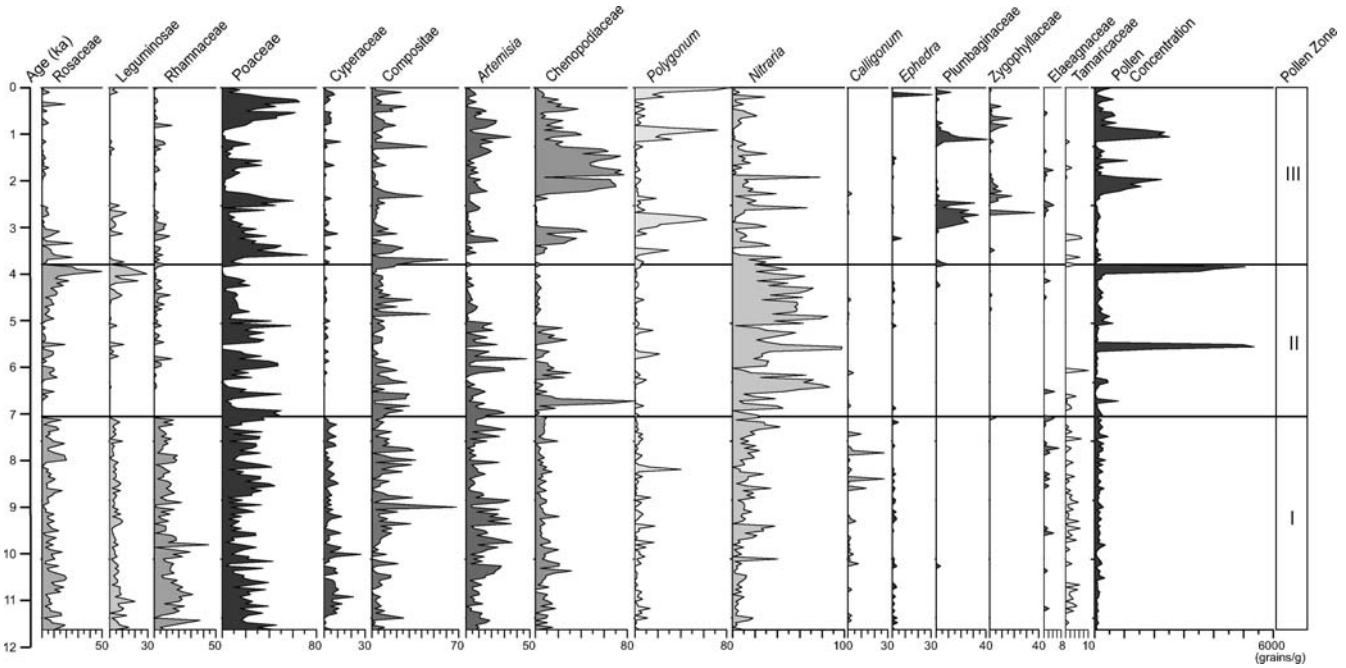

Figure 4 Pollen percentage diagram and pollen concentrations minus high-elevation and aquatic taxa

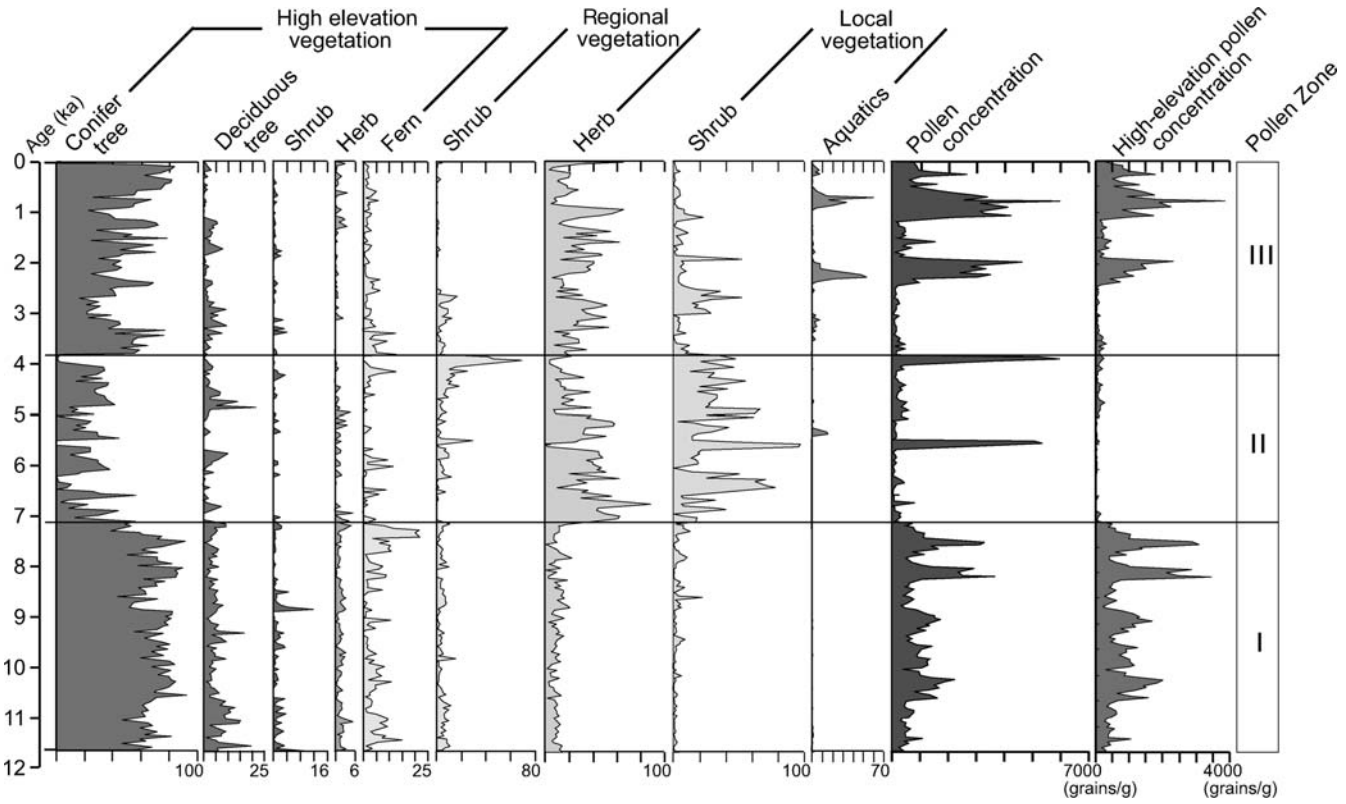

Figure 5 Pollen diagram presented as the summary of ecological groups. Pollen concentrations and pollen zones are also shown

Zone III: (152–0 cm; 3.8–0 ka)

Pollen concentrations are quite variable in this zone, ranging from 100 to 6000 grains/g (Figure 3). This zone can be divided into two main types of pollen assemblages. One is similar in character to Zone I, while the other type is similar to Zone II. In layers at 96–76 cm (2.4–1.9 ka) and 46–21 cm (1.1–0.5 ka), where the pollen concentrations are high, the pollen assemblages are similar to that of Zone I (ie, conifer pollen ranges from 38% to 80%, aquatic pollen, mainly *typha*, is relatively high, and there are corresponding reductions in lowland regional and xerophyte pollen percentages). In the layers at 152–96 cm, 76–46 cm and 21–0 cm, where the pollen concentrations are low, the pollen assemblages are similar to that of Zone II. Steppe pollen and xerophyte pollen increase and there is a corresponding decrease in aquatic pollen. Although conifer pollen ranges from 11–70%, it is mainly composed of *Sabina*, which prefers a drier climate than *Picea* (Zhu *et al.*, 2002).

Pollen concentration and *Picea–Pinus* content variations

The total pollen concentration, a proxy of vegetation density in the drainage basin as a whole, can be divided into two main stages (Figure 6). It is generally high with relatively small-range variations before 7.1 ka, but is markedly variable during the middle and late Holocene. There are four periods of low concentration, 7.1–5.0 ka, 3.4–2.4 ka, 1.9–1.2 ka and after 0.5 ka, separated by relatively high pollen concentration periods. The lowest pollen concentration occurred from 7.1 ka to 5.0 ka. Two obvious peaks in the pollen concentration curve, each lasting about 100 years, were around 5.5 ka and 3.8 ka, with both peaks resulting from increases in pollen of regional and local vegetation (Figure 4). Pollen in the first peak is mainly *Nitraria*, while that in the second is primarily Rosaceae, Leguminosae and *Nitraria*. A high-elevation pollen concentration, calculated from pollen of mountain vegetation in the drainage basin, varies in concert with the total pollen concentration (Figures 5 and 6) except during the middle Holocene. A pollen concentration calculated from local and regional vegetation has four obvious peaks during the middle and late Holocene (Figure 4). The two obvious peaks around 5.5 ka and 3.8 ka in the total pollen concentration curve are not present in the high-elevation pollen concentration curve (Figure 5). *Picea–Pinus* percentages, a proxy for high-elevation forest variation (Zhu, 2002; Zhu *et al.*, 2002), is summed from *Picea* and *Pinus* pollen in each sample. This proxy has clear variations except for a period from 7.1 ka to about 4.0 ka. Pollen concentrations and *Picea–Pinus* percentages show quite apparent millennial-scale variations (Figure 6).

Discussion

Holocene vegetation changes in the Shiyang River drainage basin

Early Holocene (11.6–7.1 ka)

At the beginning of the Holocene, conditions were favourable for pollen preservation, as evidenced by the fact that the pollen concentrations of most vegetation types, including forest, steppe and desert, are the highest for the entire Holocene. The high values of conifer pollen in the early Holocene (Figure 5) indicate the montane forest zone expanded on the north slope of the Qilian Mountains, with greater runoff causing greater transport of tree pollen (Zhu *et al.*, 2002, 2003). Since meltwater from glaciers and snow was very low in the total runoff, the high runoff in the early Holocene unlikely resulted from a warm climate, but from high precipitation under strong summer monsoon conditions. This scenario is supported by the fact that the terminal lake was larger during the early Holocene than afterward (Pachur *et al.*, 1995; Shi *et al.*, 2002).

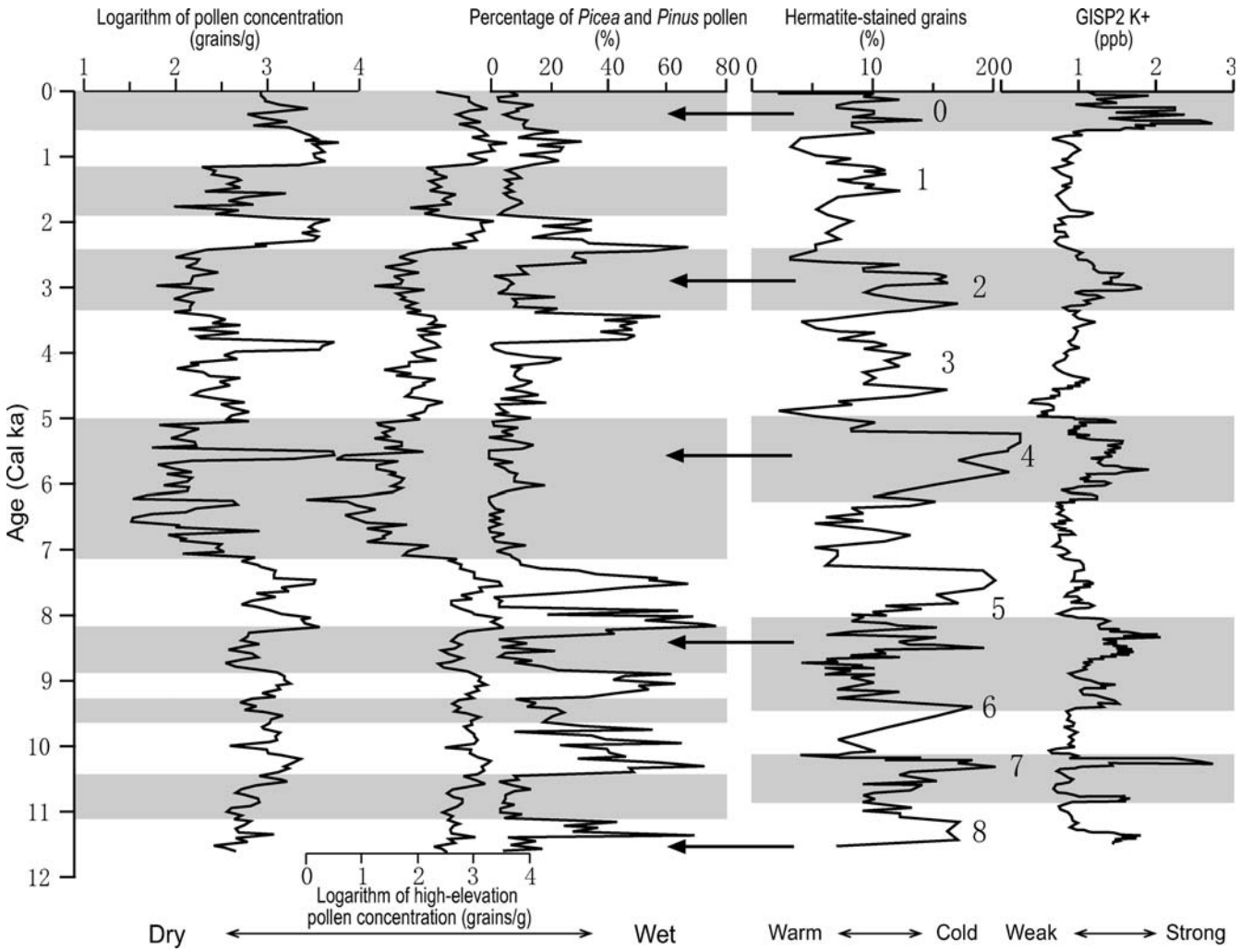

Figure 6 Correlation of total pollen concentration, high-elevation vegetation pollen concentrations, and *Picea*–*Pinus* percentages at the SJC section with percentages of hematite-stained grains in Core VM29-191 in the Northern Atlantic, an ice-raft and temperature proxy record (Bond *et al*., 2001), and potassium ion content in the GISP2 ice core, a proxy of the Siberian High (Mayewski *et al*., 1997). The episodes of high hematite-stained grain content are marked in sequence from #0–8 based on Bond *et al*. (2001). The black arrows point to the dust flux peaks in the Greenland ice core that are related to continental dry events (O'Brien *et al*., 1995). Shaded areas indicate periods of weak summer monsoon and, thus, dry climate events in the study area, and principle periods of a strong Siberian High

The pollen assemblages are also indicative of an unstable climate during the early Holocene, however, with five relatively dry periods within a generally humid background. Alternate expansion of *Picea* and *Sabina* are, respectively, indicative of a humid or a dry period (Zhu *et al*., 2002). For the early Holocene there are five periods of high *Picea* percentages at 11.6–11.1 ka, 10.4–9.7 ka, 9.3–8.8 ka, 8.2–7.9 ka and 7.8–7.3 ka (Figure 3), indicating five humid periods. During these periods, the *Picea* forest expanded in the Qilian Mountains, and *Pinus*, broadleaf trees, shrubs, herbs and ferns in the forest understorey were also better represented. Pollen concentrations are also relatively high during these periods, suggesting generally greater vegetation density in the drainage basin. The climate became relatively dry at 11.1–10.4 ka, 9.7–9.3 ka, 8.8–8.2 ka and 7.9–7.8 ka, with high *Sabina* percentages. *Picea*, *Pinus* and broadleaf forest decreased, and the forest zone at higher elevations was mainly composed of *Sabina*. Lower pollen concentrations suggest vegetation density was reduced. The low LOI content at the section during these periods (Figure 2; Chen *et al*., 2001) supports an interpretation of a low vegetation cover in the drainage and low lake production.

Mid-Holocene (7.1–3.8 ka)

During this period, desert and steppe shrubs and herbs were dominant. Low pollen concentrations suggest open vegetation and forest were reduced, with the forest belt shifting to higher elevations. The lowlands were covered primarily by steppe desert and desert vegetation. The lake area was markedly reduced between 5.6 and 5.4 ka, as suggested by very high *Nitraria* representation and a near lack of other pollen types. Two corresponding pollen concentration peaks resulted primarily from local xerophytes (Figures 4 and 5). The driest interval was from 7.0 ka, to about 5.0 ka, as evidenced by very low pollen concentrations, especially for high-elevation taxa, and low LOI content (Figure 2). There were several smaller wet oscillations during the long arid period, such as that at 4.0–3.8 ka. During these brief wet periods, vegetation cover may have increased, and there was a possible azonal desert meadow growing on the lowlands, possibly surrounding the lake.

Late Holocene (3.8–0 ka)

A *Pinus* and *Sabina* dominated forest expanded again during the late Holocene. The environment was relatively wet

compared with the mid-Holocene, but variations in pollen, sediment types and LOI content (Figure 2) indicate an alternation of dry and humid climates. However, human impacts on the environment have to be considered because of the diversion of river water for irrigation that took place during the last 2000 years (Chen *et al.*, 1999).

During relatively wet periods, such as 2.4–2.0 ka and 1.2–0.5 ka, vegetation was similar to that of the early Holocene, and vegetation cover increased in both the uplands and lowlands. Vegetation cover during these two periods may be even higher than during the early Holocene, because pollen concentration values were high for both lowland (Figure 4) and high-elevation (mountain) vegetation types (Figure 5). High aquatic plant pollen percentages, particularly *Typha*, suggest the SJC section was either submerged by shallow water or was a marshland environment. During dry periods, the vegetation cover was reduced much as during the middle Holocene, with relatively high *Sabina*, Chenopodiaceae and *Nitraria* pollen, and low LOI content suggesting relatively dry conditions. The lower reaches of the drainage basin became very dry and vegetation was dominated by Chenopodiaceae and *Nitraria*. Around 3.0 ka the lake was shallow or even dry near the section because ash and pottery of this age were found at an archaeological site 1 km away from the section. Additionally, glaciers expanded at this time and conditions were generally dry in western China (Zhou *et al.*, 1991; Huang *et al.*, 2002).

In summary, the environment of the Shiyang River drainage basin was generally wet during the early Holocene, dry during the middle Holocene, and wet but with large variations during the late Holocene. There were corresponding shifts of the montane vegetation zone along the north slope of the Qilian Mountains. The pollen concentration values also suggest millennial–centennial scale oscillations in humid climate pulses (Figures 5 and 6). During the early Holocene, vegetation density in the drainage basin increased and vegetation in high-elevation areas expanded. During the mid-Holocene, the vegetation cover was reduced, and the high forest shifted upslope. During the late Holocene, upland vegetation expanded again, but never recovered to the level of the early Holocene. The local vegetation, however, remained desert plants around the lake, consisting mainly of *Nitraria*, Plumbaginaceae, Zygophyllaceae, *Calligonum*. Desert steppe in the fluvial plain and along the banks of the river consisted of taxa such as Poaceae, Compositae, *Artemisia*, Chenopodiaceae and Rosaceae.

Monsoon evolution of the summer monsoon margin during the Holocene

In arid and semi-arid regions, precipitation and effective humidity are the main factors influencing vegetational distribution (Horowitz, 1992). In northwest China, vegetation cover is also sensitive to monsoon precipitation (Wu *et al.*, 1994; Song *et al.*, 1997; Zhu *et al.*, 2002). Because the Shiyang River drainage is situated at the maximum extent of the modern monsoon front, the variation of the summer monsoon during the Holocene can be reconstructed. Based on the pollen assemblage zones, the period 11.6–7.1 ka was marked by a relatively strong summer monsoon that brought enough precipitation to expand the terminal lake. Based on our reconstruction, the summer monsoon was weakest during the mid-Holocene (7.1–3.8 ka). The limited precipitation led to the shrinkage of the terminal lake in the drainage basin and dried other lakes in the southern Mongolian Plateau (Pachur *et al.*, 1995; Chen, F.H., *et al.*, 2003; Madsen *et al.*, 2003). In the late Holocene (3.8–0 ka), the summer monsoon strengthened, but it appears to have been weaker than during the early Holocene. Our data, therefore, suggest there were two main stages of the Holocene summer monsoon in the monsoon margin regions of China, a strong summer monsoon in the early Holocene and a generally weak summer monsoon afterward. A strong East Asian summer monsoon in the early Holocene is also evidenced by a high-resolution record of peat organic carbon isotope in northeast China (Hong *et al.*, 2005). This also indicates that the Holocene Optimum, if it even existed in China and if it is associated with the maximum strength of summer monsoon in the drainage basin, occurred much earlier than in eastern China.

Our results neither support a proposed Holocene climate optimum in the mid-Holocene, first suggested in China by Shi *et al.* (1994), nor an asynchronous Holocene Optimum of the East Asian Monsoon across China (Wu *et al.*, 1994; An *et al.*, 2000). Shi *et al.* (1994) published a synthesis of Holocene data for China, and suggested that a Holocene Optimum existed during the mid-Holocene from 8.5 to 3.0 C-14 ka BP. Since then numerous studies, including ones for the desert margin and desert-loess (Gao *et al.*, 1993), desert (Yang, 2000), lake sediments (Chen, C.T.A., *et al.*, 2003; Chen, F.H., *et al.*, 2003), and a Holocene palaeosol in the central loess plateau (Huang *et al.*, 2000), also indicate the summer monsoon was relatively strong in the early Holocene prior to *c.* 7000 cal. BP, and that a dry climate existed during the mid-Holocene in northwest China. Pollen reconstruction also suggests precipitation in semi-arid central Inner Mongolia decreased during the mid-Holocene and recovered afterwards (Wang *et al.*, 1998). More recent evidence even suggests the southern China summer monsoon was much reduced during the mid-Holocene (Zhou *et al.*, 2004). Modelling studies also predict that the southeast China monsoon would have strengthened and that west China would have become more arid during the mid-Holocene (Kutzbach and Guetter, 1986). These results, together with our data, do not support a generalized mid-Holocene climatic optimum in China.

A time-transgressive hypothesis is that China experienced a Holocene Optimum in north and northwest China before 7000 years ago, but later in south China before about 3000 years ago (Wu *et al.*, 1994; An *et al.*, 2000). That is, the East Asian summer monsoon would have decreased in intensity from the early Holocene to the present time as the monsoon front moved from north to south China (An *et al.*, 2000). However, our data suggest the Holocene in the monsoon margin region experienced two stages of strong summer monsoon with a weaker summer monsoon during the mid-Holocene. This result is very similar to lake records from south China, which indicates the Holocene experienced a dry climate and a shrinking summer monsoon from *c.* 6000 BP to 4000 BP (Zhou *et al.*, 2004). The widespread evidence for a mid-Holocene dry climate in China may indicate that the East Asian monsoon may have had a complex evolution.

Climatic events and vegetational response to millennial climatic changes during the Holocene

Relatively low pollen concentrations and low percentages of *Picea–Pinus* pollen indicate a dry climate during a weak summer monsoon, while high values indicate a wetter climate. There are seven main dry climatic periods at 0–0.5 ka, 1.2–1.9 ka, 2.4–3.4 ka, 5.0–7.1 ka, 8.3–8.8 ka, 9.2–9.7 ka and 10.4–11.2 ka (Figure 6). The primary dry climatic events are also shown in the carbonate and LOI contents (Chen *et al.*, 2001). The very high pollen concentration peaks around 5.5 ka and 3.8 ka may be due to local factors since they are

dominated by xerophytes such as Compositae and *Nitraria* as discussed above. The seven identified dry periods correlate with high percentages of the hematite-stained grains in Core VM29-19 that indicate high ice-rafted debris in the Atlantic Ocean and an association with cold climate (Bond *et al*., 2001), and with high points in the GISP2 potassium ion proxy associated with a strong Siberian High (Mayewski *et al*., 1997, 2004). The low pollen concentrations and *Picea*–*Pinus* percentages at the top of the section over the last 500 years may reflect the 'Little Ice Age', also evident in peaks in hematite-stained grains in Core VM29-19 and in the GISP2 potassium ion proxy (Figure 6). The very obvious peak (#4) of hematite-stained grains and GISP2 K^+ content (Figure 6) correlates with the strong mid-Holocene drought discussed above. There were five periods of strong Siberian High indicated by potassium ion changes during the Holocene (Figure 6; Mayewski *et al*., 2004), and high dust flux recorded in the Greenland ice core (arrows in Figure 6; O'Brien *et al*., 1995). Considering the chronological uncertainty of the age model and the resolution differences in the records, the five periods of strong Siberian High and dust flux events coincide remarkably well with the strong dry periods in our pollen record (Figure 6). Because dust in the Greenland ice comes mainly from arid central Asia, especially the arid lands of northwestern China (Biscaye *et al*., 1997), and because a strong Siberian High eventually results in a strong winter monsoon and a dry, dusty climate, the five high dust-influx and Siberian High events should also indicate five periods of marked dry climate in arid and semi-arid China during the Holocene. During the Holocene, the hematite-stained grain proxy indicates nine episodes of strong cold climate (#0–8 beside the hematite-stained grain curve in Figure 6). Although the #3 event is not well documented in our pollen record, and there are slight chronological differences in cold events recorded in the early Holocene, all of the cold climatic events in the North Atlantic are well represented as dry climate events in this continental interior terminal lake. However, it should also be noted that although the climatic events documented by the hematite-stained grain proxy from the North Atlantic core, the GISP2 K^+ content and our pollen proxy at the SJC section correlate well, there are also obvious differences. The #1 hematite-stained grain cold event peak is not reflected in the GISP2 K^+ Siberian High proxy, although a dry climate is documented in our SJC section at the time. The #3 hematite-stained grain peak is recorded in neither the GISP2 K^+ proxy nor our pollen assemblage. Our pollen assemblage records a longer dry period in the mid-Holocene than either of the GISP2 K^+ and the hematite-stained grain records. The pollen assemblage at the SJC section documents a humid, but variable, early Holocene climate with three marked dry episodes (Figure 6), a record that is similar to the hematite-stained grain proxy but different from the GISP2 K^+ proxy. The differences among the records may indicate complex responses of the East Asian Monsoon, the Siberian-Mongolian High, and ice-drift intensity in the North Atlantic to temperature changes possibly induced by solar variations (Bond *et al*., 2001). The different time-resolutions and chronological accuracies of the three geological records may also make correlation difficult. Although differences exist among the three records, the climatic changes in high latitude records and Eurasian continental interior are more similar than different. Therefore, our pollen data from the SJC section supports at least hemispheric, if not global, climatic event correlations at multicentennial to millennial timescales during the Holocene.

Conclusions

(1) Our high-resolution pollen record from the Eurasian continental interior of arid China is characterized by three major pollen assemblage zones during the Holocene: from a mountain forest zone dominated by *Sabina*, *Picea,* and *Pinus* 11.6–7.1 ka, to a mixed desert and steppe lowland zone dominated by *Nitraria*, Poaceae, Compositae, *Artemisia* and Chenopodiaceae 7.1–3.8 ka, to a forest-steppe zone dominated by *Sabina*, *Pinus*, Poaceae, *Artemisia* and Chenopodiaceae 3.8–0 ka. These shifts in pollen assemblages likely reflect both elevation shifts in vegetation belts along the north slope of the Qilian Mountains and change in the amount of vegetation cover in the drainage basin.
(2) The vegetation shifts were in response to change in effective moisture. The wet climate in the early Holocene corresponds with a Holocene monsoon maximum for the region. The Holocene Optimum in the drainage was in the early Holocene, and differs from East China where the Holocene Optimum may have been in the middle Holocene, if it existed at all. Our results show that the East Asian summer monsoon was weak in the mid-Holocene, resulting in a very dry climate from 7.1 ka to 5.0 ka, but recovered in the late Holocene after about 5 ka.
(3) The pollen record at the SJC section reflects millennial- and centennial-scale climatic changes. This regularity appears to be persistent during the moist and dry phases of the Holocene, suggesting pervasive and sensitive moisture responses to climate changes in the continental interior during the Holocene. Our record supports indications of high latitude and middle latitude correlations for climatic events at multicentennial and millennial timescales.

Acknowledgements

We thank Q. Shi and H.B. Wu for fieldwork and Professor J.X. Cao for laboratory work. This paper is a special contribution in the memory of author Dr Yan Zhu who conducted most of the pollen analysis. We give special thanks to John Dodson and another anonymous reviewer who made constructive suggestions and improved the English text. The field investigations were supported by China International Collaboration Project 2002CB714004 and an NSFC grant (No. 40271116). The laboratory analysis was supported by the NSFC Innovation Team Project (No. 40421101) and special NSFC grant (No. 40125001).

References

An, C.B., Feng, Z.D. and **Tang, L.Y.** 2003: Evidence of a humid mid-Holocene in western part of Chinese Loess Plateau. *Chinese Science Bulletin* 48, 2472–79.
An, Z.S., Porter, S.C., Kutzbach, J.E., Wu, X.H., Wang, S.M., Liu, X.D., Li, X.Q. and **Zhou, W.J.** 2000: Asynchronous Holocene optimum of the East Asian monsoon. *Quaternary Science Reviews* 19, 743–62.
Bianchi, G.G. and **McCave, I.N.** 1999: Holocene periodicity in North Atlantic climate and deep-ocean flow south of Iceland. *Nature* 397, 515–17.
Biscaye, P.E., Grousset, F.E., Revel, M., Van der Gaast, S., Zielinski, G.A., Vaars, A. and **Kukla, G.** 1997: Asian provenance of glacial dust (stage 2) in the Greenland Ice Sheet Project 2 ice core, Summit, Greenland. *Journal of Geophysical Research* 102, 26 765–81.

Bond, G., Showers, W., Cheseby, M., Lotti, R., Almasi, P., deMenocal, P., Priore, P., Cullen, H., Hajdas, I. and **Bonani G.** 1997: A pervasive millennial-scale cycle in the North Atlantic Holocene and glacial climate. *Science* 278, 1257–66.

Bond, G., Kromer, B., Beer, J., Muscheler, R., Evans, M.N., Showers, W., Hoffmann, S., Lotti-Bond, R., Hajdas, I. and **Bonani, G.** 2001: Persistent solar influence on North Atlantic Climate during the Holocene. *Science* 294, 2130–36.

Campbell, I.D., Campbell, C., Apps, M.J., Rutter, N.W. and **Bush, A.B.G.** 1998: Late Holocene ~1500 year climatic periodicities and their implication. *Geology* 26, 471–73.

Chen, C.T.A., Lan, H.C., Lou, J.Y. and **Chen, Y.C.** 2003: The dry Holocene Megathermal in Inner Mongolia. *Palaeogeography Palaeoclimatology Palaeoecology* 193, 181–200.

Chen, F.H., Shi, Q. and **Wang, J.M.** 1999: Environmental changes documented by sedimentation of Lake Yiema in arid China since the last glaciation. *Journal of Paleolimnology* 22, 159–69.

Chen, F.H., Zhu, Y., Li, J.J., Shi, Q., Jin, L.Y. and **Wünemann, B.** 2001: Abrupt Holocene changes of the Asian monsoon at millennial- and centennial-scales: evidence from lake sediment document in Minqin Basin, NW China. *Chinese Science Bulletin* 46, 1942–47.

Chen, F.H., Wu, W., Holmes, J.A., Madsen, D.B., Zhu, Y., Jin, M. and **Oviatt C.G.** 2003: A mid-Holocene drought interval as evidenced by lake desiccation in the Alashan Plateau, Inner Mongolia China. *Chinese Science Bulletin* 48, 1401–10.

Chen, L.H. and **Qu, Y.G.** 1992: *Water resource and land use in Hexi region*. Chinese Science Press, 15–25.

Cheng, B. 2002: A preliminary study on pollen assemblage of surface samples in Shiyang River Drainage, NW China. Masters Thesis, Lanzhou University, Lanzhou, China.

Cheng, B., Zhu, Y., Chen, F.H., Zhang, J.W., Huang, X.Z. and **Yang, M.L.** 2004: Relationship between the surface pollen and vegetation in Shiyang River drainage, Northwest China. *Journal of Glaciology and Geocryology* 26, 81–88 (in Chinese, with English abstract).

Dansgaard, W., Johnsen, S.J., Clausen, H.B., Dahl-Jensen, D., Gundestrup, N.S., Hammer, C.U., Hvidberg, C.S., Steffensen, J.P., Sveinbjörnsdottir, A.E., Jouzel, J. and **Bond, G.** 1993: Evidence for general instability of past climate from a 250-kyr ice-core record. *Nature* 364, 218–20.

Feng, Z.D., Chen, F.H., Zhang, H.C. and **Ma, Y.Z.** 2000: Contribution to global change of Mongolian Plateau and Loess Plateau in the last glaciation and interglacial period. *Journal of Desert Research* 20, 171–77 (in Chinese, with English abstract).

Gao, S.Y., Chen, W.N., Jin, H.L., Dong, G.R., Li, B.S., Jin, J. and **Liu, L.Y.** 1993: Preliminary study on the Holocene desert evolution in the NW boundary of the Asia monsoon. *Science in China, Series D* 23, 202–209 (in Chinese).

Gao, Y.X., Xu, S.Y., Guo, Q.R. and **Zhang, M.L.** 1962: Monsoon region and regional climate of China. In Gao, Y.X. and Xu, S.Y., editors, *Some problems of East Asian Monsoon*. Chinese Science Press, 49–63 (in Chinese).

He, Y.Q., Theakstone, W.H., Zhang, Z.L., Zhang, D.A., Yao, T.D., Chen, T., Shen, Y.P. and **Pang, H.X.** 2004: Asynchronous Holocene climatic change across China. *Quaternary Research* 61, 52–63.

Hong, Y.T., Hong, B., Lin, Q.H., Shibata, Y., Hirota, M., Zhu, Y.X., Leng. X.T., Wang, Y., Wang, H. and **Yi, L.** 2005: Inverse phase oscillations between the East Asian and Indian Ocean summer monsoons during the last 12 000 years and paleo-El Niño. *Earth and Planetary Science Letters* 231, 337–46.

Horowitz, A. 1992: *Palynology of arid lands.* Elsevier, 1–530.

Huang, C.C., Zhou, J., Pang, J.L., Han, Y. and **Hou, C.H.** 2000: A regional aridity phase and its possible cultural impact during the Holocene Megathermal in the Guanzhong Basin, China. *The Holocene* 10, 135–42.

Huang, C.C., Pang, J.L. and **Li, P.H.** 2002: Abruptly increased climatic aridity and its social impact on the Loess Plateau of China at 3100 a BP. *Journal of Arid Environments* 52, 87–99.

Huang, D.X. 1997: *Gansu vegetation.* Gansu Science and Technology Press, 163–67 (in Chinese).

Jouzel, J., Lourius, C., Petit, J.R., Genthon, C., Barkov, N.I., Kotlyakov, V.M. and **Petrov, V.M.** 1987: Vostok ice core: a continuous isotope temperature record over the last climatic cycle (160 000 years). *Nature* 329, 403–408.

Kutzbach, J.E. and **Guetter, P.J.** 1986: The influence on changing orbital parameters and surface boundary condition on climate simulation for the past 18 000 years. *Journal of the Atmospheric Sciences* 43, 1726–59.

Li, G.Y., Qian, Z.S. and **Hu, J.** 1995: *Palynological analysis manual.* Geological Publishing House, 1–212.

Li, X.Q., Zhou, W.J., An, Z.S. and **Dong, G.R.** 2000: The palaeovegetation record of monsoon evolution in the desert–loess transition zone for the last 13 ka BP. *Acta Botanica Sinica* 42, 868–72 (in Chinese, with English abstract).

Liu, X.Q., Shen, J. and **Wang, S.M.** 2002: A 16 000-year pollen record of Qinghai lake and its paleoclimate and paleoenvironment. *Chinese Science Bulletin* 47, 1391–96.

Ma, Y.Z., Zhang, H.C., Pachur, H.J., Wünnemann, B., Li, J.J. and **Feng, Z.D.** 2004: Modern pollen-based interpretations of mid-Holocene palaeoclimate (8500 to 3000 cal. BP) at the southern margin of the Tengger Desert, northwestern China. *The Holocene* 14, 841–50.

Madsen, D.B., Chen, F.H., Oviatt, C.G., Zhu, Y., Brantingham, P.J., Elston, R.G. and **Bettinger, R.L.** 2003: Late Pleistocene/Holocene wetland events recorded in southwest Tengger Desert lake sediments, NW China. *Chinese Science Bulletin* 48, 1423–29.

Mayewski, P.A., Meeker, L.D., Twickler, M.S., Whitlow, S., Yang, Q.Z., Lyons, W.B. and **Prentice, M.** 1997: Major features and forcing of high-latitude northern hemisphere atmospheric circulation using a 110 000-year-long glaciochemical series. *Journal of Geophysical Research* 102, 26 345–66.

Mayewski, P.A., Rohling, E.E., Stager, J.C., Karlén, W., Maasch, K.A., Meeker, L.D., Meyerson, E.A., Gasse, F., van Kreveld, S., Holmgren, K., Lee-Thorp, J., Rosqvist, G., Rack, F., Staubwasser, M., Schneider, R.R. and **Steig, E.J.** 2004: Holocene climate variability. *Quaternary Research* 62, 243–55.

O'Brien, S.R., Mayewski, P.A., Meeker, L.D., Meese, D.A., Twickler, M.S. and **Whitlow, S.I.** 1995: Complexity of Holocene climate as reconstructed from a Greenland ice core. *Science* 270, 1962–64.

Pachur, H.J., Wünnemann, B. and **Zhang, H.** 1995: Lake evolution in the Tengger desert, northwestern China, during the last 40 000 years. *Quaternary Research* 44, 171–80.

Shi, Q., Chen, F.H., Zhu, Y. and **Madsen, D.** 2002: Lake evolution of the terminal area of the Shiyang River drainage in arid China since the last glaciation. *Quaternary International* 93–94, 31–43.

Shi, Y.F., Kong, Z.C., Wang, S.M., Tang, L.Y., Wang, F.B., Yao, T.D., Zhao, X.T., Zhang, P.Y. and **Shi, S.H.** 1994: Climates and environments of the Holocene megathermal maximum in China. *Science in China (Series B)* 37, 481–93.

Song, C.Q., Lu, H.Y. and **Sun, X.J.** 1997: Establishment of transfer function of the pollen-climate factors in northern China and the application. *Chinese Science Bulletin* 42, 2182–86 (in Chinese).

Stager, J.C. and **Mayewski, P.A.** 1997: Abrupt early to mid-Holocene climate transition registered at the equator and the poles. *Science* 276, 1834–36.

Stuiver, M. and **Reimer, P.J.** 1993: Extended C-14 data-base and revised CALIB 3.0 C-14 age calibration program. *Radiocarbon* 35, 215–30.

Von Grafenstein, U., Erlenkeuser, H., Brauer, A., Jouzel, J. and **Johnsen, S.J.** 1999: A mid-European Decadal isotope-climate record from 15 500 to 5000 years B.P. *Science* 284, 1654–57.

Wang, F.Y., Song, C.Q., Cheng, G.Q. and **Sun, X.J.** 1998: Palaeoclimate reconstruction by adopting the pollen-climate response surface model to analysis of the Chasuqi deposition section. *Acta Botanica Sinica* 40, 1067–74 (in Chinese, with English abstract).

Wu, X.H., An, Z.S., Wang, S.M., Liu, X.D., Li, X.Q., Zhou, W.J., Liu, J.F., Lu, J.J., Porter, S.C. and **Kutzbach, J.E.** 1994: The temporal and spatial variation of East-Asian Summer Monsoon in Holocene optimum in China. *Quaternary Science* 1, 24–37 (in Chinese, with English abstract).

Yang, X.P. 2000: Landscape evolution and precipitation changes in the Badain Jaran desert during the last 30 000 years. *Chinese Science Bulletin* 45, 1042–47.
Zhang, H.C., Ma, Y.Z., Wünnemann, B. and **Pachur, H.J.** 2000: A Holocene climatic record from arid northwestern China. *Palaeogeography Palaeoclimatology Palaeoecology* 162, 389–401.
Zhou, S.Z., Chen, F.H., Pan, B.T., Cao, J.X. and **Li, J.J.** 1991: Environmental changes during the Holocene in the Western China on Millennial time scale. *The Holocene* 1, 151–56.
Zhou, W.J., Yu, X.F., Jull, A.J.T., Burr, G., Xiao, J.Y., Lu, X.F. and **Xian, F.** 2004: High-resolution evidence from southern China of an early Holocene optimum and a mid-Holocene dry event during the past 18 000 years. *Quaternary Research* 62, 39–48.
Zhu, Y. 2002: The Holocene pollen from the lake sediments and environmental changes in the Shiyang River drainage, arid China. Ph.D. Thesis, Lanzhou University, Lanzhou, China.
Zhu, Y., Chen, F.H. and **Madsen, D.** 2002: The environmental signal of an early Holocene pollen record from the Shiyang River basin lake sediments, NW China. *Chinese Science Bulletin* 47, 267–73.
Zhu, Y., Xie, Y.W., Cheng, B., Chen, F.H. and **Zhang, J.W.** 2003: Pollen transport in the Shiyang River drainage, arid China. *Chinese Science Bulletin* 48, 1499–506.